Non-isothermal crystallization of PCL/CLAY nanocomposites

Matias R. Lanfranconi, Vera A. Alvarez and Leandro N. Ludueña*

[1]Thermoplastic Composite Materials Group (CoMP), Research Institute of Material Science and Technology (INTEMA), National Research Council (CONICET), Engineering Faculty, Mar del Plata University, Av. Colón 10890 (7600) Mar del Plata, Argentina

*Corresponding author

Abstract

In this work, Differential Scanning Calorimetry (DSC) was used to study the crystallization behavior of nanocomposites based on polycaprolactone (PCL) reinforced with organo-montmorillonite (C20A) and organo-bentonite (B-THBP) under non-isothermal conditions. The effect of clay content (0.0, 2.5, 5.0 and 7.5 wt.%) was analysed. Linear and non-linear regression methods were used to calculate theoretical kinetic parameters. The study was focused on the correlation between the non-isothermal crystallization process and the morphology of the clay inside the PCL matrix. Continuous cooling transformation diagrams were obtained by means of a mathematical model that involves both induction and growth of the crystal during cooling. For the construction of these diagrams, both crystallization steps, crystals induction (analysed by the induction time equation) and growing (studied by a crystal growth model), were considered. Copyright © 2018 VBRI Press.

Keywords: Non-isothermal crystallization, kinetic models, biodegradable polymers, organo-clays, nanocomposites.

Introduction

The main industry of polymer processing is related with packaging whereas the food industry is its principal customer. The major part of polymer packaging is based on traditional polymers and represents millions of tons per year, thus became the design of biodegradable polymeric products of great importance [1]. It is known that Polycaprolactone (PCL) is one of these kinds of polymer. PCL is linear, hydrophobic and partially crystalline polyester that can be slowly consumed by micro-organisms [1] and exhibits the additional advantage that processing techniques such as extrusion, injection molding and film blow molding can be used to obtain a final product [1-4]. Nevertheless, it presents also several drawbacks, being the worst one its low stiffness which can be overcome by the incorporation of layered silicates to the polymer matrix [4-7].

Polymer/layered silicate nanocomposites consist on inorganic nanoparticles dispersed in the polymeric matrix [8-11]. Great improvements of mechanical, thermal, barrier and physical properties of the different polymer matrices have been obtained by the incorporation of these kinds of fillers at very low contents (less than 10wt.%), especially when the length to diameter ratio of the silicates is large [12-14-16]. Crystallization parameters of the neat matrix, such as crystallite size and morphology, crystallinity degree and crystallization kinetic, are often affected by the incorporation of fillers [17]. Many studies can be found in the literature dealing with the effect of inorganic fillers or reinforcements on the crystallization behavior of different polymer matrices [17]. However, dissimilar or contradictory tendencies were found studying the crystallization rate of partially crystalline polymers in the presence of nanoclays [18, 11, 19-23].

The final quality and performance of polymer products depends on the crystalline morphology developed during processing; which involves melting and crystallization during cooling. So that, it is necessary to recognize the parameters that affects the crystallization behavior in order to optimize the processing conditions looking for the required properties of the final product. Both isothermal and non-isothermal experiments can be performed to study the crystallization behavior of polymer matrices. The crystallization behavior is often studied under idealized situations at which external conditions are constant in order to simplify the theoretical analysis. These studies do not simulate real processing stages which involve a continuous changing environment. Typical cases are polymer cooling stages in industrial processing lines. Increasing the complexity of the theoretical treatment of the crystallization behavior applied to industrial processing techniques has been the objective of many scientific researchers whom have proposed several non-isothermal crystallization kinetic models applied to neat matrices to nanocomposites [24-26].

The aim of this work was to experimentally study the effect of the type and content of clay on the non-isothermal crystallization behavior of polycaprolactone. A global kinetic model for the analysis and design of

real processing operations will be proposed. The correlation between the clay dispersion degree inside the polymeric matrix and the non-isothermal behavior of the studied nanocomposites will be carefully analyzed.

Theoretical background: Kinetics crystallization models

The evolution of crystallinity as a function of temperature can be expressed as the relative degree of crystallinity, $\alpha(T)$:

$$\alpha(T) = \int_{T_o}^{T} ((\partial Hc/\partial T)dT) \Bigg/ \int_{T_o}^{T_\infty} ((\partial Hc/\partial T)dT) \tag{1}$$

where T_o and T_∞ are the onset and final crystallization temperatures, respectively; and H_c is the crystallization enthalpy.

The classical Avrami equation [27-30] has been applied to the crystallization kinetics of polymer matrices under isothermal conditions and also for composites and nanocomposites. The general form of the Avrami equation is expressed as follows:

$$\alpha(t) = 1 - \exp(-k.t^n) \tag{2}$$

where n is the Avrami exponent, which depends on the nucleation mechanism and the geometry of crystal growth, and k is the overall kinetic constant, which includes nucleation parameters as well as growth-rate parameters.

Some authors have adapted the Avrami model for non-isothermal processes by discretization to small isothermal intervals [30-33]. Ozawa [31] was the first author dealing with this approach and it was applied to several polymeric materials [34-36]. Avrami modified model was written as [37-40]:

$$1 - \alpha = \exp\left(-K(T)/\phi^m\right) \tag{3}$$

where $K(T)$ is a function of cooling rate; ϕ is the cooling rate and m is the Ozawa exponent depending on the crystal growth. Applying natural logarithm two times to both sides of Equation (3) the following equation is obtained:

$$\ln(-\ln(1-\alpha)) = \ln(K(T)) - m.\ln\phi \tag{4}$$

$K(T)$ and m can be calculated by the linear regression of the plot $\ln(-\ln(1-\alpha))$ as a function of $ln\phi$, at a given temperature. Another possibility is the non-linear regression to obtain these values. This method deals with the early stages of crystallization ($40\% > \alpha(T) > 10\%$), in order to avoid problems arising from the effects of secondary crystallization process. Values of $\alpha(T)$ at a given temperature for different cooling rates are required in the Osawa model. Hence, the range of cooling rates and temperatures that can be applied is narrow. It can be concluded that Ozawa's model assumes constant cooling rate, so it cannot be applied to predict the evolution of crystallinity under real processing conditions.

For all studied models, k generally can be expressed as an Arrhenius type equation [34, 41-43, 33]:

$$k = k_0 \exp\left(\frac{Ea}{R(Tm^0 - T)}\right) \tag{5}$$

where k_0 is the pre-exponential factor; Ea is the activation energy, Tm^0 is the theoretical melting point and R is the gas constant. Due to the fact that crystallization rate is zero at Tm^0; the factor $1/(Tm^0-T)$ can be considered as the thermodynamic driving force for the crystallization process.

It must be taken into account that the n and $K(T)$ parameters in non-isothermal analysis do not have the same physical meaning as in the isothermal one. Jeziorny [33] modified the isothermal Avrami's model to the non-isothermal one by defining the rate parameter Zt as a function of cooling rate as follows:

$$\ln Zc = \ln Zt / \phi \tag{6}$$

where Zc is the corrected kinetic rate constant.

Mo [44] developed a method to describe the non-isothermal crystallization process taking into account the physical variables relating to the process: the relative degree of crystallinity (α), the cooling rate (ϕ), and the crystallization temperature (T_c). Both equations can be related as follows:

$$\ln Zt + n \ln t = \ln K(T) - m \ln \phi \tag{7}$$

by rearrangement at a given crystallinity, α, the equation is converted into:

$$\ln \phi = \ln F(T) - a \ln t \tag{8}$$

where $F(T)=[K(T).Z_t^{-1}]^{1/m}$ refers to the cooling rate, and $a = n.m^{-1}$ is the ratio between the Avrami's to the Ozawa's exponent.

It is known that the crystallization temperature changes as a function of cooling rate. Friedman [45] proposed the differential iso-conversional method to evaluate the effective energy barrier for the non-isothermal crystallization which can be expressed as follows:

$$\ln(d\alpha/dt) = A - \Delta E_a/RT \tag{9}$$

where $d\alpha/dt$ is the crystallization rate for a given α, A is an arbitrary factor and ΔE_a is the effective energy barrier of the process for a given α.

Thus the relative crystallinity as a function of time, $\alpha(t)$, is differentiated to obtain the crystallization rate as a function of time. Then, ΔE_a can be calculated from the slope of the linear regression of the plot $ln\ (d\alpha/dt)$, measured at various cooling rates, as a function of the inverse temperature for a given relative crystallinity.

Nucleation activity

Dobreva et al. [46] has proposed a model for quantifying the nucleation activity (φ) of different substrates during the non-isothermal crystallization of polymer melts. The nucleation activity tends to zero

when the substrate is extremely active, while it is close to one for inert substrates. At temperatures close to melting, the cooling rate for nucleation from the melt can be expressed as follows:

$$\ln(\phi) = A - (B / \Delta T_c^2) \qquad (10)$$

where ϕ is the cooling rate, A is a constant, $\Delta T_c = T_m - T_c$ is undercooling degree, T_c is the crystallization temperature, T_m is the melting temperature and B is a parameter related to the three dimensional nucleation. The value of B for the pure polymer and its composites (B^*) can be obtained from Equation (10). Then, φ can be calculated by Eq. (11)

$$\varphi = B^* / B \qquad (11)$$

Experimental

Materials/ chemicals details

Raw materials

Polycaprolactone (PCL) with a number molecular weight Mn=80000 was purchased from Sigma Aldrich. The reinforcements used were Cloisite 20A (C20A) and bentonite supplied by Southern Clay Products and Minarmco S.A., respectively. C20A was used as received. Tributylhexadecylphosphonium (TBHP) bromide supplied by Sigma Aldrich was used as organo-modifier of bentonite.

Material synthesis / reactions

Modification of bentonite with tributil hexadecyl phosphonium bromide

A solution of 2.5 g of bentonite dispersed in 100 ml of deionized water was prepared. Then, an aqueous solution of TBHP of the corresponding concentration (0.9 times the cation exchange capability of the bentonite) was added. The mixture was stirred for 4 hours at 70ºC. After that, the suspension was filtered through a Buchner Funnel and washed with deionized water until free of bromide. The wet organoclay, named B-TBHP, was frozen for 24 hours and then lyophilized at 100 mTorr and −50 °C for 72 hours using a VirTis 2KBTES-55 freeze dryer.

The main properties of the used organo-clays are shown in **Table 1.**

Table 1. Properties of organo-clays.

Clay	Organic Modifier	Abs. water 24h at 90% RH (%)	d_{001} (nm)	Weight loss on ignition (%)	Tp TGA (° C)
B-TBHP	$CH_3(CH_2)_3$—$\overset{(CH_2)_3CH_3}{\underset{(CH_2)_3CH_3}{\overset{|}{C}}}$—$(CH_2)_{15}CH_3$	2.73	2.51	29	388.7
C20A	H_3C—$\overset{CH_3}{\underset{HT}{\overset{|}{N^+}}}$—HT	3.72	2.42	41	303.1

Preparation of nanocomposites

PCL was intercalated in 2.5, 5.0 and 7.5 wt.% of each clay by melt blending in a Brabender type mixer at

100°C and 150r.p.m. for 10min. Then, sheets with a thickness in the range of 0.3 to 5.0mm were prepared by compression molding in a hydraulic press. The procedure used was 5 min at 100ºC without pressure, 5min at 100°C and 50kg/cm², mold cooling with water circuits until achieving room temperature maintaining 50kg/cm² and finally mold opening.

Characterizations / device fabrications /response measurements

Differential Scanning Calorimetry

Modulated differential scanning calorimetry was used to study the bulk-crystallization process of the materials. The equipment used was a MDSC Q2000 RCS90 TA Instruments. Tests were done under nitrogen atmosphere. The following temperature program was applied to 10.0 ± 0.1 mg of each sample:

1. Heating from 0 ℃ to 100 ℃ at 10 ℃/min.
2. Melting at 100 ℃ for 10 minutes.
3. Cooling to initial temperature at several rates (from 5 to 40 ℃/min).

Results and discussion

Effect of clay content and clay type on the crystallization process of PCL

Fig. 1 shows the MDSC curves of PCL and their nanocomposites with 5 wt.% of each clay, for different cooling rates.
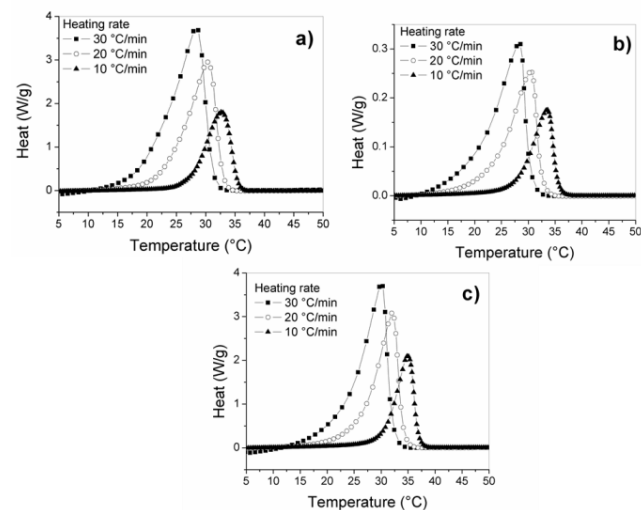
Fig. 1. Cold crystallization curves at several cooling rates for: a) PCL; b) PCL + 5 wt.% C20A and c) PCL + 5 wt.% B-TBHP.

Similar curves were obtained for all studied systems. The exothermic peak temperature (T_P) and the onset crystallization temperature (T_o) were obtained from these curves. All parameters are reported in **Table 2.**

T_p and T_o shift to lower temperatures as a function of the cooling rate as a consequence of its effect on the nucleation process. Increasing cooling rate means shorter time periods for the same temperature range.

Therefore, higher undercooling degree is required to initiate crystallization [30]. It is clear from the previous table that whereas C20A produce a decrease on the crystallization temperature, especially at low contents, B-TBHP makes that crystallization to start at higher temperatures. This last effect can be attributed to particles of B-THBP having a heterogeneous nucleation effect on PCL macromolecule segments. In the molten state, PCL macromolecule segments can be easily physically attached to the surface of the B-TBHP particle, which leads to the crystallization of PCL molecules at higher crystallization temperature [47].

The obtained results could be also be related with the clay dispersion degree inside the polymeric matrix, which was previously studied by X-ray diffraction [48]. The initial basal spacing or interlayer distance (d_{001}) of each neat clays are reported in **Table 1**. Studying the nanocomposites, basal spacing of the clay was larger for PCL/C20A than PCL/B-TBHP nanocomposites at the same clay content. This result confirms the improved intercalation of PCL chains inside the C20A platelets [49]. Analyzing the effect of clay content, a decrease on the d_{001} for 5 wt.% as compared with 2.5 wt.% for C20A was also found. This effect could be associated with the partial agglomeration of clay platelets at higher clay contents [50]. Then a slight increase of the interlaminar space for nanocomposites with 7.5 wt.% of C20A was also observed. The B-TBHP nanocomposites showed the same tendency [50].

The effect of clay type and content on the non-isothermal induction and half-crystallization times, at different cooling rates, is shown in **Table 2**.

Table 2. Relevant parameters of crystallization process of PCL/clay nanocomposites.

T_p: Temperature of the peak (ºC)							
Cooling rate (ºC/min)	PCL	2.5C20A	5C20A	7.5C20A	2.5TBHP	5TBHP	7.5TBHP
10	32.6	28.8	33.6	31.7	36.3	34.8	36.2
20	30.3	25.1	30.7	28.5	33.7	32.0	33.4
30	28.7	22.5	28.6	25.7	31.9	30.3	31.7
T_i: Temperature of the initial crystallization (ºC)							
Cooling rate (ºC/min)	PCL	2.5C20A	5C20A	7.5C20A	2.5TBHP	5TBHP	7.5TBHP
10	36.0	34.4	37.2	39.1	39.2	39.0	40.0
20	33.9	31.4	34.3	36.5	36.8	35.5	36.0
30	33.6	29.5	32.8	33.5	35.7	32.7	34.4
Induction time							
Cooling rate (ºC/min)	PCL	2.5C20A	5C20A	7.5C20A	2.5TBHP	5TBHP	7.5TBHP
10	0.18	0.22	0.175	0.50	0.22	0.19	0.08
20	0.10	0.11	0.1	0.28	0.1	0.08	0.07
30	0.08	0.08	0.08	0.05	0.08	0.02	0.04
Half-crystallization time							
Cooling rate (ºC/min)	PCL	2.5C20A	5C20A	7.5C20A	2.5TBHP	5TBHP	7.5TBHP
10	0.40	0.65	0.50	0.84	0.46	0.49	0.32
20	0.25	0.40	0.30	0.49	0.28	0.25	0.25
30	0.23	0.30	0.23	0.31	0.23	0.15	0.19
Parameters of the modelling of induction time							
Parameter	PCL	2.5C20A	5C20A	7.5C20A	2.5TBHP	5TBHP	7.5TBHP
ln Ktind	-10.222	-8.224	-7.356	-14.773	-9.071	-17.371	-7.19
Etind/R (K)	265.39	234.35	168.92	457.28	206.78	459.55	129.77
tind (△T=35ºC)	0.07	0.22	0.08	0.18	0.04	0.014	0.03

Parameters of Avrami's models for matrix and nanocomposites							
	10 ºC/min			20 ºC/min			
	n	ln Zt	Zc	n	ln Zt	Zc	
PCL	1.99	1.36	1.17	1.99	2.30	1.22	
PCL + 5 wt.% C20A	2.91	1.77	1.14	2.60	2.89	1.18	
PCL + 5 wt.% B-TBHP	3.42	2.16	1.13	2.61	3.36	1.15	

Parameters of Ozawa's model for matrix and nanocomposites obtained at several temperatures						
Temperature (ºC)	PCL		PCL + 5 wt.% C20A		PCL + 5 wt.% B-TBHP	
	m	ln k	m	ln k	m	ln k
32	2.60	5.48	3.10	6.72	2.51	7.17
30	2.47	6.08	2.70	5.07	1.84	6.61
28	1.51	4.30	1.81	3.46	1.05	4.86
26	1.22	3.86	1.26	3.33	0.94	3.94
24	0.88	3.22	0.88	2.59	0.58	3.29

Parameters of Mo's model for matrix and nanocomposites obtained at several temperatures						
Relative crystallinity	PCL		PCL + 5 wt.% C20A		PCL + 5 wt.% B-TBHP	
	a	ln F(T)	a	ln F(T)	a	ln F(T)
0.2	2.12	-0.74	1.30	0.79	0.76	1.50
0.4	1.81	0.38	1.40	1.10	0.90	1.57
0.6	1.85	0.88	1.40	1.47	1.06	1.66
0.8	1.80	1.51	1.42	1.49	1.22	1.94

Nucleation activity obtained by Dobreva's method							
	PCL	2.5C20A	5C20A	7.5C20A	2.5TBHP	5TBHP	7.5TBHP
Nucleation activity (φ)	1	1.09	1.37	1.30	1.63	1.41	1.63

The determination of non-isothermal induction time must be analyzed considering the difference between onset temperature and theoretical melting point (To -Tm0) but in this case it was previously demonstrated [48] that the thermodynamic melting point was practically unchanged by the incorporation of both clays (Tm0 = 63.8 ± 0.6 ºC). For all clay concentrations used in the present work, the influence of B-TBHP platelets as nucleating agent dominates with respect to the retardant one [43-44].

The effect of nanoclay content on induction time (t_{ind}, defined as the time needed for the formation of the equilibrium nucleus with critical dimensions at a given T [54]) and half-crystallization time ($t_{1/2}$) was also analyzed. Jiménez et al. [51] studied the crystallization process of PCL/organically modified clay nanocomposites. Clay acted as nucleation agent when low contents of it were added to the matrix. Otherwise, increasing clay content hinders the transportation of polymer segments retarding the crystallization process in comparison with the neat matrix [51]. The same trend was observed for polyethylene-oxide/MMT [52] and Nylon6/MMT [53] nanocomposites. In our case, the analysis became harder due to the differences in the crystallization temperature that drive to different driving forces. The induction time was calculated for all materials. The t_{ind} is considered the most representative macroscopic parameter of the nucleation process in differential scanning calorimetry experiments [55]. Some studies have proposed the following relationship of tind with temperature:

$$t_{ind} = K_{tind} \cdot \exp\left(\frac{E_{tind}}{R.\Delta T}\right) \quad (12)$$

where K_{tind} is the preexponential factor, E_{tind} is the activation energy, R is universal gas constant and $\triangle$T is undercooling degree (defined as $T_m^0 - T_c$).

The parameters K_{tind} and E_{tind} were calculated from the linear regression of the plots $ln\ t_{ind}$ as a function of $\triangle T^{-1}$. The results are summarized in **Table 2**. The linear dependence between $ln\ t_{ind}$ and $\triangle T^{-1}$ implies that there were not changes in the morphology of the nuclei during crystallization. From the obtained parameters it is possible to determine the induction time for a given undercooling degree. **Table 2** also includes the values calculated for $\triangle$T = 35ºC. From this table, by analyzing the effect of clay content, it can be observed that nanocomposites with C20A produce a clear increase in the induction time which could be related with the higher dispersion degree reached in this kind of nanocomposites. On the other hand, the B-TBHP nanocomposites showed the opposite trend, i.e. tind decreased for nanocomposites which can be related with the fact that clay agglomerates could be acting as heterogeneous nucleation points. Similar trends were observed for the half crystallization times (from which the overall crystallization time can be estimated). The half crystallization time is shorter as a function of undercooling degree and became longer as a function of clay dispersion degree. Krikorian et al. [56] have

proposed the hypothesis that when the clay dispersion degree is higher, the clay layers may hinder the chain-folding mechanism for local poly(L-lactic acid) crystallization. So, both theories (clays acting as nucleation agents decreasing both tind and t½ and clays hindering the chains folding mechanism increasing both tind and t½) could be competing to give the observed result regarding the effect of clay compatibility and clay content on the crystallization behavior of PCL matrix.

Fig. 2 show the relative degree of crystallinity as a function of temperature, at 10 °C/min, for matrix and nanocomposites.
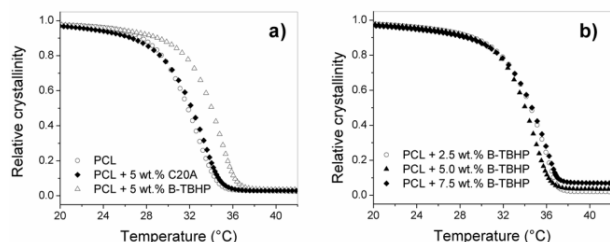
Fig. 2. Relative degree of crystallinity as a function of temperature at 10 °C/min, for: a) PCL matrix and nanocomposites with 5 wt.% of C20A and B-TBHP and b) PCL + 2.5; 5.0 and 7.5 wt.% of B-TBHP nanocomposites.

From **Fig. 2 a**, it is clear that the incorporation of 5 wt.% of organo-modified bentonite (B-TBHP) displayed an accelerating effect (crystallization from the melt started at higher temperatures) on the crystallization process of PCL whereas the effect of C20A not meaningful, which could be attributed to the dissimilar compatibility of each clay with the PCL matrix. On the other hand, **Fig. 2 b** shows that the crystallization behavior of nanocomposites is not significantly modified changing the clay content. Similar tendencies were observed in the case of C20A.

Kinetic models: Crystallization process prediction

Fig. 3 show the relative degree of crystallinity as a function of time, for matrix and nanocomposites.
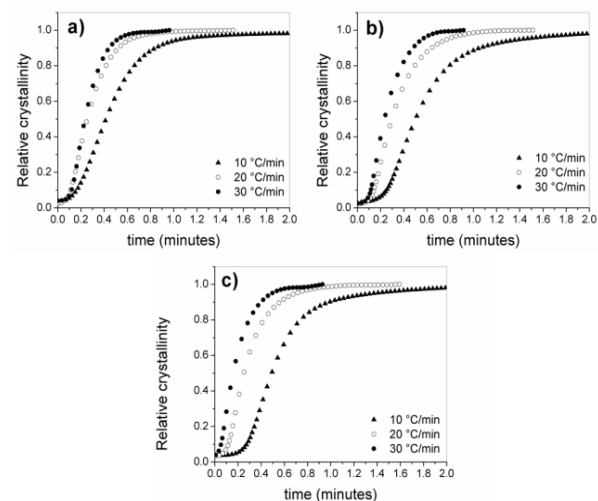
Fig. 3. Relative degree of crystallinity as a function of time at 10 °C/min, for: a) PCL b) nanocomposites with 5 wt.% of C20A and c) nanocomposites with 5 wt.% of B-TBHP.

Independently of the used model, the accuracy of the modeled data is worst as a function of the cooling rate. This result can be attributed to heat transference to the sample, diffusion and secondary crystallization, which are phenomena that usually take place at high cooling rates and relative degree of crystallinity higher than 0.8 [57].

The theoretical parameters calculated from the application of Avrami's model to the studied systems are summarized in **Table 2**. The extension of Jeziorny was also applied and Zc is also included in that table. It must be noted that the parameters Z_t and n do not have the same physical meaning in isothermal and non-isothermal crystallization because the continuous changing temperature in the latter. This phenomenon affects both nucleation and growth processes. In this case, Z_t and n are two adjustable parameters which are used to fit the experimental results.

The exponent n in non-isothermal crystallization showed a wide range of values. Even so, n for PCL/clay was larger than that for PCL matrix at all studied cooling rates. This result confirms that non-isothermal crystallization of PCL/clay is developed with tridimensional growth and heterogeneous nucleation. For all materials (matrix and nanocomposites), the value of Z_c slightly decreased as a function of cooling rate. It is also important to note that these models (Avrami and Jeziorny) were not able to reproduce the crystallization curves for the complete range of relative crystallinity degrees by means of one set of parameters (n and Z_c).

It can be seen that the curves in the plots of ln (−ln(1−α)) *vs.* lnϕ for PCL and PCL/organo-clays nanocomposites (**Fig. 4**) did not exhibit an excellent linear relationship.
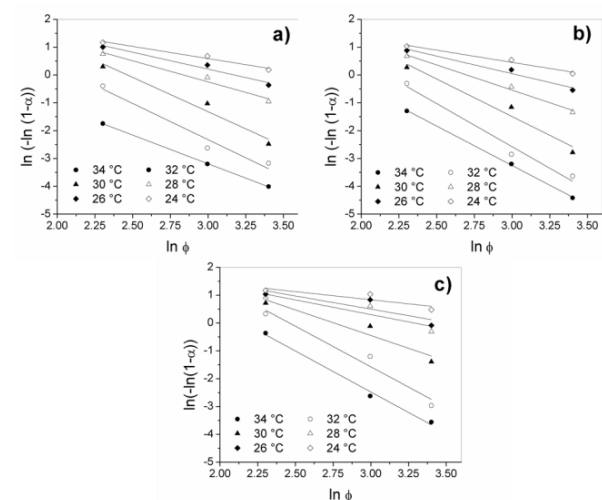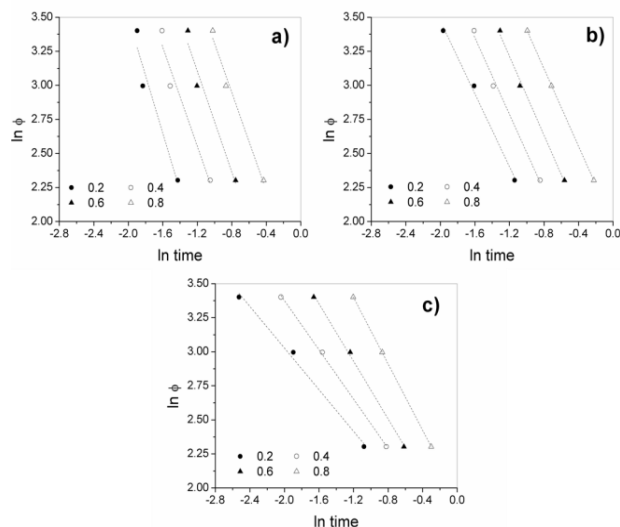

Fig. 4. Plots of $\ln(-\ln(1-\alpha))$ vs $ln\phi$ (Ozawa's model) obtained at different constant temperatures for: a) PCL b) nanocomposites with 5 wt.% of C20A and c) nanocomposites with 5 wt.% of B-TBHP.

It can be attributed to the fact that the crystallization processes at a given temperature and different cooling rates take place at different stages, i.e., crystallization at lower cooling rate is toward the end of

the process, whereas crystallization process at higher cooling rate stays at an earlier stage. Nevertheless, it was possible to determine global parameters of Ozawa's model at different temperatures and the results are also summarized on **Table 2**. It can be seen from this table that the Ozawa exponent *m* increases as a function of temperature for all materials. On the other hand, the Ozawa rate constant k(T) decreases as a function of temperature, which means that the material crystallizes slower at higher temperature (lower driving force for the crystallization process) [58]. The nanocomposites with the organobentonite (B-TBHP) showed higher K(T) values than the neat PCL, at any given crystallization temperature, which is in accordance with all previous results. The opposite behavior was shown for nanocomposites with C20A which can be attributed to the clay dispersion degree inside the PCL matrix.

Fig. 5 show the application of Mo's model at different crystallinity degrees for matrix and nanocomposites. The parameters obtained from the linear regression of $\ln\phi$ *vs.* $\ln t$ are displayed in **Table 2.**

Fig. 5. Plots of *lnϕ* vs. *ln time* (Mo's model) obtained at different constant relative crystallinity degrees (0.2, 0.4, 0.6 and 0.8) for: a) PCL b) nanocomposites with 5 wt.% of C20A and c) nanocomposites with 5 wt.% of B-TBHP.

The value of *a* for PCL matrix was near to 1.8, and decreased for PCL/clay nanocomposites. On the other hand, *F*(*T*) increased as a function of the relative degree of crystallinity. For a given relative degree of crystallinity, *F*(*T*) for PCL/BTBHP is higher than that for PCL matrix, which indicates that PCL/BTBHP crystallizes at a faster rate than PCL. The obtained results can also be associated with the clay dispersion degree inside the PCL matrix.

The values of the nucleation activity are shown in **Table 2**. The behavior observed for the nucleation activity is in accordance with the tendencies obtained from the model's parameters used to fit the experimental non-isothermal crystallization process of the nanocomposites.

The nucleation and growth of crystals for a specific cooling condition can be estimated from the phase diagrams [41, 59]. The most common used diagrams are the time-temperature transformations plots (TTT, isothermal processes) and the continuous-cooling transformations plots (CCT, constant cooling rate) in which the crystallinity is related with *t* and *T* at a constant cooling rate. These methods are useful to improve the knowledge about the entire crystallization behavior [59-61]. CCT plots of all samples are shown on **Fig. 6** where curves representing different relative degree of crystallization are plotted as a function of time. The points of these plots have been calculated by integration of the full model (nucleation and growth) at a given cooling rate. When a certain curve of relative degree of crystallization is intercepted by a constant cooling rate curve, the resulting point corresponds to the time needed to reach a specific degree of crystallization under those thermal conditions.
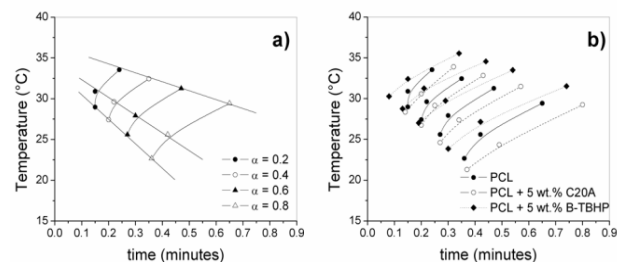
Fig. 6. CCT diagram for: a) PCL matrix and b) PCL matrix and nanocomposites with 5 wt.% of each clay (C20A and B-TBHP).

It can be seen from **Fig. 6** that for B-TBHP nanocomposites lower times are required to reach the onset of crystallization and relative crystallinity degree of 0.5. This result is in accordance with the previous analysis confirming that this clay acts as effective nucleating agent. In the case of the C20A nanocomposites, a slight effect on the onset crystallization time was observed.

Conclusion

The non-isothermal crystallization behavior of polycaprolactone with different organo-modified clay contents was studied. The most important effects of the layered silicate were related with the retardant effect of both clays on the crystallization process of PCL matrix. The full model was also used to prepare the CCT diagram of crystallization. This diagram is useful for the calculation of the crystallinity degree at different processing conditions which is an important tool for process design and optimization. This diagram allows showing adequately the retardant effect of different clays and contents in the sample.

Author's contributions

Conceived the plan: VA; Performed the exepirments: ML; Data analysis: ML, LL, VA; Wrote the paper: LL, VA. Authors have no competing financial interests.

Supporting information

Supporting informations are available from VBRI Press.

References

1. Lepoittevin B, Pantoustier N, Devalckenaere M, Alexandre M, Kubies D, Calberg C et al. Poly (ε-caprolactone)/clay nanocomposites by in-situ intercalative polymerization catalyzed by dibutyltin dimethoxide. Macromolecules. 2002; 35(22):8385-90.
   DOI: 10.1021/ma020300w
2. Kunioka M, Ninomiya F, Funabashi M. Novel evaluation method of biodegradabilities for oil-based polycaprolactone by naturally occurring radiocarbon-14 concentration using accelerator mass spectrometry based on ISO 14855-2 in controlled compost. Polymer Degradation and Stability. 2007; 92(7):1279-88.
   DOI: 10.1016/j.polymdegradstab.2007.03.028
3. Lepoittevin B, Pantoustier N, Devalckenaere M, Alexandre M, Calberg C, Jérôme R et al. Polymer/layered silicate nanocomposites by combined intercalative polymerization and melt intercalation: a masterbatch process. Polymer. 2003; 44 (7): 2033-40.
   DOI: 10.1016/S0032-3861(03)00076-4
4. Luduena LN, Alvarez VA, Vazquez A. Processing and microstructure of PCL/clay nanocomposites. Materials Science and Engineering: A. 2007; 460:121-9.
   DOI: 10.1016/j.msea.2007.01.104
5. Luduena L, Kenny J, Vázquez A, Alvarez V. Effect of clay organic modifier on the final performance of PCL/clay nanocomposites. Materials Science and Engineering: A. 2011; 529:215-23.
   DOI: 10.1016/j.msea.2011.09.020
6. Ollier R, Lanfranconi M, Ludueña L, Alvarez V, editors. Preparation and Characterization of PCL/Modified-Clay Biodegradable Nanocomposites Euporean Polymer Conference EPF 2013 2013 2013; Pisa.
7. Ludueña L, Vázquez A, Alvarez V. Effect of the type of clay organo-modifier on the morphology, thermal/mechanical/ impact/barrier properties and biodegradation in soil of polycaprolactone/clay nanocomposites. Journal of Applied Polymer Science. 2013;128(5):2648-57.
   DOI: 10.1002/app.38425
8. Messersmith PB, Giannelis EP. Synthesis and barrier properties of poly (ε-caprolactone)-layered silicate nanocomposites. Journal of Polymer Science Part A: Polymer Chemistry. 1995; 33 (7):1047-57.
   DOI: 10.1002/pola.1995.080330707
9. Kojima Y, Usuki A, Kawasumi M, Okada A, Fukushima Y, Kurauchi T et al. Mechanical properties of nylon 6-clay hybrid. Journal of Materials Research. 1993; 8(05):1185-9.
   DOI: 10.1557/JMR.1993.1185
10. Usuki A, Kojima Y, Kawasumi M, Okada A, Fukushima Y, Kurauchi T et al. Synthesis of nylon 6-clay hybrid. Journal of Materials Research. 1993;8(05):1179-84.
   DOI: 10.1557/JMR.1993.1179
11. Perez C, Vázquez A, Alvarez V. Isothermal crystallization of layered silicate/starch-polycaprolactone blend nanocomposites. Journal of Thermal Analysis and Calorimetry. 2008; 91(3):749-57. **DOI:** 10.1007/s10973-007-8213-6
12. Hu X, Zhao X. Effects of annealing (solid and melt) on the time evolution of polymorphic structure of PA6/silicate nanocomposites. Polymer. 2004; 45(11):3819-25.
   DOI: 10.1016/j.polymer.2004.03.055
13. Kawasumi M, Hasegawa N, Kato M, Usuki A, Okada A. Preparation and mechanical properties of polypropylene-clay hybrids. Macromolecules. 1997; 30(20):6333-8.
   DOI: 10.1021/ma961786h
14. Lee H-S, Fishman D, Kim B, Weiss R. Nano-composites derived from melt mixing a thermotropic liquid crystalline polyester and zinc sulfonated polystyrene ionomers. Polymer. 2004; 45(23):7807-11.
   DOI: 10.1016/j.polymer.2004.09.049
15. Alexandre M, Dubois P. Polymer-layered silicate nanocomposites: preparation, properties and uses of a new class of materials. Materials Science and Engineering: R: Reports. 2000; 28(1):1-63. **DOI:** 10.1016/S0927-796X(00)00012-7
16. Viville P, Lazzaroni R, Pollet E, Alexandre M, Dubois P, Borcia G et al. Surface characterization of poly (ε-caprolactone)-based nanocomposites. Langmuir. 2003; 19(22):9425-33.
   DOI: 10.1021/la034723i
17. Kennedy M, Brown G, St-pierre L. The effect of silica on the crystallization of isotactic poly (propylene oxide). Polymer Composites. 1984; 5(4):307-11.
   DOI: 10.1002/pc.750050410
18. Papageorgiou GZ, Achilias DS, Bikiaris DN, Karayannidis GP. Crystallization kinetics and nucleation activity of filler in polypropylene/surface-treated SiO 2 nanocomposites. Thermochimica Acta. 2005; 427 (1):117-28.
   DOI: 10.1016/j.tca.2004.09.001
19. Ludueña LN, Vazquez A, Alvarez VA. Crystallization of polycaprolactone–clay nanocomposites. Journal of Applied Polymer Science. 2008;109 (5):3148-56.
   DOI: 10.1002/app.28266
20. Rong MZ, Zhang MQ, Pan SL, Lehmann B, Friedrich K. Analysis of the interfacial interactions in polypropylene/silica nanocomposites. Polymer International. 2004; 53(2):176-83.
   DOI: 10.1002/pi.1307
21. Papageorgiou GZ, Achilias DS, Bikiaris DN. Crystallization Kinetics of Biodegradable Poly (butylene succinate) under Isothermal and Non-Isothermal Conditions. Macromolecular Chemistry and Physics. 2007; 208(12):1250-64.
   DOI: 10.1016/j.polymdegradstab.2009.01.009
22. Yang F, Ou Y, Yu Z. Polyamide 6/silica nanocomposites prepared by in situ polymerization. Journal of Applied Polymer Science. 1998; 69(2):355-61.
   DOI: 10.1002/(SICI)1097-4628(19980711)69:2<355::AID-APP17>3.0.CO;2-V
23. Li Y, Yu J, Guo ZX. The influence of interphase on nylon-6/nano-SiO2 composite materials obtained from in situ polymerization. Polymer international. 2003; 52(6):981-6.
   DOI: 10.1002/pi.1173
24. Xu W, Liang G, Zhai H, Tang S, Hang G, Pan W-P. Preparation and crystallization behaviour of PP/PP-g-MAH/Org-MMT nanocomposite. European Polymer Journal. 2003; 39(7):1467-74.
   DOI: 10.1016/S0014-3057(03)00015-6
25. Kim SH, Ahn SH, Hirai T. Crystallization kinetics and nucleation activity of silica nanoparticle-filled poly (ethylene 2, 6-naphthalate). Polymer. 2003; 44(19):5625-34.
   DOI: 10.1016/S0032-3861(03)00623-2
26. Rong MZ, Zhang MQ, Zheng YX, Zeng HM, Walter R, Friedrich K. Structure–property relationships of irradiation grafted nano-inorganic particle filled polypropylene composites. Polymer. 2001; 42(1):167-83.
   DOI: 10.1016/S0032-3861(00)00325-6
27. Liu X, Wu Q. Non-isothermal crystallization behaviors of polyamide 6/clay nanocomposites. European Polymer Journal. 2002; 38(7):1383-9.
   DOI: 10.1016/S0014-3057(01)00304-4
28. Avrami M. Kinetics of phase change. I General theory. The Journal of Chemical Physics. 1939;7(12):1103-12.
   DOI: 10.1063/1.1750380
29. Avrami M. Kinetics of phase change. II transformation-time relations for random distribution of nuclei. The Journal of Chemical Physics. 1940; 8(2):212-24.
   DOI: 10.1063/1.1750631
30. Avrami M. Granulation, phase change, and microstructure kinetics of phase change. III. The Journal of Chemical Physics. 1941; 9(2):177-84.
   DOI: 10.1063/1.1750872

31. Ozawa T. Kinetics of non-isothermal crystallization. Polymer. 1971; 12 (3):150-8.
DOI: 10.1016/0032-3861(71)90041-3
32. Nakamura K, Katayama K, Amano T. Some aspects of nonisothermal crystallization of polymers. II. Consideration of the isokinetic condition. Journal of Applied Polymer Science. 1973; 17(4):1031-41.
DOI: 10.1002/app.1973.070170404
33. Jeziorny A. Parameters characterizing the kinetics of the non-isothermal crystallization of poly (ethylene terephthalate) determined by DSC. Polymer. 1978; 19(10):1142-4.
DOI: 10.1016/0032-3861(78)90060-5
34. Vyazovkin S. Isoconversional Kinetic Analysis of Thermally Stimulated Processes in Polymers. Macromolecular Rapid Communications. 2006; 27(18): 1515-1532.
DOI: 10.1002/marc.200600404
35. Pérez C, Alvarez V, Stefani P, Vázquez A. Non-isothermal crystallization of Materbi-Z/clay nanocomposites. Journal of Thermal Analysis and Calorimetry. 2006; 88(3):825-32.
DOI: 10.1007/s10973-005-7466-1
36. Bogdanov B. Isometric crystallization of stretched poly (e-caprolactone) sheets for medical applications. Journal of Thermal Analysis and Calorimetry. 2003; 72(2):667-74.
DOI: 10.1023/A:1024502421970
37. Medeiros E, Tocchetto R, Carvalho L, Conceição M, Souza A. Nucleating effect and dynamic crystallization of a poly (propylene)/attapulgite system. Journal of Thermal Analysis and Calorimetry. 2002; 67(2):279-85.
DOI: 10.1023/A:1013946310044
38. De Medeiros E, Tocchetto R, De Carvalho L, Santos I, Souza A. Nucleating effect and dynamic crystallization of a poly (propylene)/talc system. Journal of Thermal Analysis and Calorimetry. 2001;66(2):523-31.
DOI: 10.1023/A:1013121102536
39. Hu A-M, Liang K-M, Wang G, Zhou F, Peng F. Effect of nucleating agents on the crystallization of Li2O-Al2O3-SiO2 system glass. Journal of Thermal Analysis and Calorimetry. 2004;7 8 (3):991-7.
DOI: 10.1007/s10973-005-0465-0
40. Chrissafis K, Efthimiadis K, Polychroniadis E, Chadjivasiliou S. Crystallization kinetics of amorphous. Journal of Thermal Analysis and Calorimetry. 2003; 74(3):761-7.
DOI: 10.1023/B:JTAN.0000011008.82102.52
41. Di Lorenzo M, Silvestre C. Non-isothermal crystallization of polymers. Progress in Polymer Science. 1999; 24(6):917-50.
DOI: 10.1016/S0079-6700(99)00019-2
42. Chan T, Isayev A. Quiescent polymer crystallization: modelling and measurements. Polymer Engineering & Science. 1994; 34(6):461-71.
DOI: 10.1002/pen.760340602
43. Maffezzoli A, Kenny J, Nicolais L. A macrokinetic approach to crystallization modelling of semicrystalline thermoplastic matrices for advanced composites. Journal of materials science. 1993; 28(18):4994-5001.
DOI: 10.1007/BF00361167
44. Liu T, Mo Z, Wang S, Zhang H. Nonisothermal melt and cold crystallization kinetics of poly (aryl ether ether ketone ketone). Polymer Engineering & Science. 1997; 37(3):568-75.
DOI: 10.1002/pen.11700
45. Vyazovkin S, Sbirrazzuoli N. Isoconversional analysis of calorimetric data on nonisothermal crystallization of a polymer melt. The Journal of Physical Chemistry B. 2003; 107(3):882-8.
DOI: 10.1021/jp026592k
46. Dobreva A, Gutzow I. Activity of substrates in the catalyzed nucleation of glass-forming melts. II. Experimental evidence. J Non-Cryst Solids. 1993; 162(1):13-25.
DOI: 10.1016/0022-3093(93)90737-I
47. Xu W, Zhai H, Guo H, Zhou Z, Whitely N, Pan W-P. PE/Org-MMT nanocomposites. Journal of Thermal Analysis and Calorimetry. 2004; 78(1):101-12.
DOI: 10.1023/B:JTAN.0000042158.70250.39
48. Lanfranconi M, Alvarez V, Ludueña L. Isothermal crystallization of polycaprolactone/modified clay biodegradable nanocomposites. Journal of Thermal Analysis and Calorimetry. 2016; 126:1273-1280. **DOI:** 10.1007/s10973-016-5734-x
49. Wagener R, Reisinger TJ. A rheological method to compare the degree of exfoliation of nanocomposites. Polymer. 2003; 44 (24):7513-8.
DOI: 10.1016/j.polymer.2003.01.001
50. Ollier R, Lanfranconi M, Ludueña L, Alvarez V. Preparation and characterization of PCL/modified-clay biodegradable nanocomposites. Euporean polymer conference EPF 2013; Pisa.
51. Jimenez G, Ogata N, Kawai H, Ogihara T. Structure and thermal/mechanical properties of poly (ε-caprolactone)-clay blend. Journal of Applied Polymer Science. 1997; 64(11):2211-20.
DOI: 10.1002/(SICI)1097-4628(19970613)64:11<2211::AID-APP17>3.0.CO;2-6
52. Homminga D, Goderis B, Dolbnya I, Reynaers H, Groeninckx G. Crystallization behavior of polymer/montmorillonite nanocomposites. Part I. Intercalated poly (ethylene oxide)/ montmorillonite nanocomposites. Polymer. 2005; 46 (25): 11359-65.
DOI: 10.1016/j.polymer.2005.10.016
53. Fornes T, Paul D. Crystallization behavior of nylon 6 nanocomposites. Polymer. 2003; 44 (14):3945-61.
DOI: 10.1016/S0032-3861(03)00344-6
54. Janevski A, Bogoeva-Gaceva G. Isothermal crystallization of iPP in model glass-fiber composites. Journal of Applied Polymer Science. 1998; 69 (2):381-9.
DOI: 10.1002/(SICI)1097-4628(19980711)69:2<381::AID-APP20>3.0.CO;2-Y
55. Torre L, Maffezzoli A, Kenny JM. A macrokinetic approach to crystallization applied to a new thermoplastic polyimide (New TPI) as a model polymer. Journal of Applied Polymer Science. 1995; 56(8):985-93.
DOI: 10.1002/app.1995.070560812
56. Krikorian V, Pochan DJ. Unusual crystallization behavior of organoclay reinforced poly (L-lactic acid) nanocomposites. Macromolecules. 2004; 37(17): 6480-91.
DOI: 10.1021/ma049283w
57. Xu T, Wang Q, Fan Z. Non-Isothermal crystallization kinetics of exfoliated and intercalated polyethylene/montmorillonite nanocomposites prepared by in situ polymerization. European Polymer Journal 2005; 41: 3011–3017.
DOI: 10.1016/j.eurpolymj.2005.04.042
58. Jiao C, Wang Z, Liang X, Hu Y. Non-isothermal crystallization kinetics of silane crosslinked polyethylene. Polymer Testing. 2005; 24 (1):71-80.
DOI: 10.1016/j.polymertesting.2004.07.007
59. Spruiell JE, White JL. Structure development during polymer processing: Studies of the melt spinning of polyethylene and polypropylene fibers. Polymer Engineering & Science. 1975; 15(9):660-7.
DOI: 10.1002/pen.760150905
60. Hsiung C, Cakmak M, Ulcer Y. A structure oriented model to simulate the shear induced crystallization in injection moulded polymers: a Lagrangian approach. Polymer. 1996; 37(20):4555-71.
DOI: 10.1016/0032-3861(96)00291-1
61. Ulcer Y, Cakmak M, Miao J, Hsiung C. Structural gradients developed in injection-molded syndiotactic polystyrene (sPS). Journal of Applied Polymer Science. 1996; 60(5):669-91.
DOI: 10.1002/(SICI)1097-4628(19960502)60:5<669::AID-APP4>3.0.CO;2-O